ELSEVIER

Biochemical Engineering Journal 37 (2007) 80–85

Biochemical Engineering Journal

www.elsevier.com/locate/bej

A simple and accurate method for simulation of hollow fiber biocatalyst membrane reactors

Elio E. Gonzo, Juan C. Gottifredi *

Instituto de Investigaciones para la Industria Química (INIQUI-CONICET), Universidad Nacional de Salta, Facultad de Ingeniería, Buenos Aires 177, A4402 FDC Salta, Argentina

Received 12 April 2006; received in revised form 20 March 2007; accepted 25 March 2007

Abstract

A recently developed technique to estimate effectiveness factor in catalytic pellets [J.C. Gottifredi, E.E. Gonzo, On the effectiveness factor calculation for a reaction-diffusion process in an immobilized biocatalyst pellet, Biochem. Eng. J. 24 (2005) 235–242] is used to greatly simplify the simulation of membrane biocatalyst reactors. The whole problem is reduced to well-known plug flow packed bed reactor after an appropriate definition of an effectiveness factor (η) that takes into account chemical consumption in the catalytic region and mass transfer resistances of the reactive component. A standard R–K routine can then be applied since, at each mesh point, η is calculated through a non-linear algebraic equation.

Results produced with this procedure compare fairly well with previous findings. Moreover some experimental results of kinetics studies related with enzyme immobilization are used to simulate membrane hollow fiber reactors and conversion, concentrations and η profiles along reactor axial position.

The procedure can be applied to any biocatalytic system provided a single chemical reaction takes place although the kinetic expression can be arbitrary.

Keywords: Hollow fiber reactor; Effectiveness factor; Mass transport resistances; Immobilized enzyme; Reactor simulation

1. Introduction

An increasing interest related to the use of purified enzymes as biocatalysts in laboratory and industrial scale is being developed as a new group of technologies suitable to fill the growing needs of more safe chemical processes [1–4]. Since 1971, when Rony [5,6], suggested "immobilizing" enzyme within the spongy matrix of hollow fiber membranes, several techniques to immobilize the enzyme in the hollow fiber, as well as, suitable reactor were presented [3,7,8].

Asymmetric hollow fiber membranes provide a suitable support for enzyme immobilization. These reactors are usually conformed by a bundle of tubes. The spongy matrix structure, where enzymes are supported, is confined between tube impermeable walls and a very thin skin – around 5 μm thick – of dense polymer or porous ceramic which allows reactive and products mass transfer but being impermeable to enzyme large molecules. The resulting reaction region where conversion takes place by catalytic action is usually 70 μm thick. Thus chemicals must diffuse from the stream flow to the reaction zone and products back to the stream trough the dense polymer or ceramic barrier. As a consequence several mass transfer series resistances must be considered with simultaneous chemical reaction to simulate reactor behavior.

In this type of reactors, although conversion increases along the axial position under steady-state conditions, the reaction only takes place in the spongy region causing a concentration radial gradient of the key reactive component that must be balanced by the diffuse radial flux at the wall of the lumen region. As a consequence the simulation of reactor behavior requires, at each axial position, the estimation of the key component consumption in the spongy region. Thus a non-linear second order differential equation defined by boundary values must be solved at each axial position of the reactor. This is not an easy task even with modern numerical techniques specifically when steep concentration profiles arise due to fast specific reaction rates. Moreover since the actual lumen concentration at the end of each step must be estimated the resulting non-linear differential equation

* Corresponding author.
E-mail address: gottifre@unsa.edu.ar (J.C. Gottifredi).

1369-703X/$ – see front matter © 2007 Elsevier B.V. All rights reserved.
doi:10.1016/j.bej.2007.03.011

Nomenclature

a	distance from center tube to lumen–membrane interface (Fig. 1) (m)
b	distance from center tube to spongy region–membrane interface (Fig. 1) (m)
B	parameter defined by Eq. (4) (mol/m s)
C	concentration (mol/m^3)
C_0	mixed cup concentration in the lumen (mol/m^3)
C^*	dimensionless concentration defined by Eq. (11b)
d	tube radius (Fig. 1) (m)
D_{ef}	effective diffusivity (m^2/s)
F^o	key component entrance molar feed rate (mol/s)
K	partition coefficient
k_L	liquid phase mass transfer coefficient (m/s)
K_m	Michaelis–Menten kinetic parameter (Eq. (22)) (mol/m^3)
L	reactor length (m)
P	dimensionless parameter defined by Eq. (17)
r	radial coordinate (m)
R	intrinsic reaction rate (mol/m^3 s)
R^*	dimensionless rate of reaction (see Eq. (11))
R_V	spongy region to total reactor volume ratio
V_m	maximum rate of Michaelis–Menten equation (see Eq. (22)) (mol/m^3 s)
x	reactor radial coordinate (m)
X	key component reaction conversion
z	reactor axial coordinate (m)

Greek letters

α	parameter given by (b/d)
δ	parameter defined by Eq. (19)
η	effectiveness factor defined by Eq. (13)
ϕ	Thiele modulus defined by Eq. (12)
ϕ^*	modified Thiele modulus defined by Eq. (17)
ρ	parameter defined by Eq. (18)
σ	parameter defined by Eq. (19)
Ω	bioreactor total cross section (m^2)

Subscripts

a	denotes concentration at $r=a$
am	denotes concentration in equilibrium at $r=a$
b	denotes concentration at $r=b$
bm	denotes concentration in equilibrium at $r=b$
m	denotes diffusivity in the skin membrane

Superscript

0	denotes concentration at reactor entrance ($z=0$)

must be solved more than once at each point grid of the axial position.

A number of attempts have been reported in the literatures [9–14] to find a close solution of the resulting design equations. However, the intrinsic nonlinearity of the governing mass balance differential equation for the key species in the system does not permit an analytical solution. Therefore a numerical method must be applied to solve the system, which cannot be easily applied, especially for the effectiveness factor calculation in the spongy biocatalyst region where the reaction rate takes place.

Waterland et al. [13] obtained the exact analytical expression for substrate concentration profile through an idealized fiber assuming first order biocatalytic kinetic reaction. The resulting expression, however, is not suitable for straightforward calculations; therefore a numerical technique, based on finite difference, has also been used in their contribution to account for non-linear kinetic expressions. Kim and Cooney [21] presented a close solution strictly valid when the reaction kinetics is well described by a first order irreversible expression. In the last years several contributions have been presented among which Jayaraman and Kulkarni [11] can be cited. After defining an effectiveness factor based on lumen concentration at the wall, the authors solved the problem as a linear Graetz model but where one of the boundary condition (at the wall) is function of reactor position. Thus a Volterra type integro differential equation was generated by the superposition principle which was solved numerically step by step along the reactor. However, in each step the flux at the wall due to reaction must be evaluated which requires the numerical solution of the diffusion reaction differential equation. More recently, Cabrera et al. [9] used Green's functions to obtain the general solution of the mass balance differential equations. The derived integral equations had to be numerically solved on an approximately transformed coordinate system. Uniform rectangular grids on the original coordinate system were used to solve the equations. Sousa and Mendes [12] presented a new numerical scheme using orthogonal collocation together with an independent variable transformation (spatial coordinate) to solve the model equations associated with catalytic membrane reactors. The new scheme is claimed to avoid the imprecise results obtained when traditional numerical methods such as finite differences with equispaced intervals or orthogonal collocation are used.

The purpose of this contribution is to show that a previous procedure recently presented by the authors [15], is a powerful and appropriate tool to overcome all numerical problems associated with instabilities and stiffness of the non-linear diffusion reaction differential equation. Instead a truly algebraic approach is used at each point of the axial coordinate of a plug flow steady-state reactor to simulate the performance of an actual biocatalytic reactor as shown below. Numerical conversion values are compared with previous findings showing excellent agreement. Finally the reactor performances of real systems, with potential industrial interest, are simulated to show reactor behavior through concentration profiles in each region and the resulting effectiveness factor evolution along the axial coordinate.

2. Hollow fiber bioreactor model

A conventional hollow fiber bioreactor is considered in this analysis. A schematic representation of the reactor is shown in Fig. 1. Reactants are fed through the inner tube (known as the lumen) from where they can diffuse through the thin skin membrane to the outer annular region (spongy matrix) where

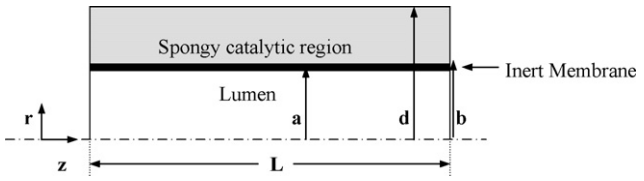

Fig. 1. Schematic representation of the hollow fiber reactor.

the reaction occurs with the enzyme biocatalyst therein. The thin skin membrane being permeable to reactants and products but impermeable to the high molecular weight enzyme. Products diffuse back through the membrane to the lumen and flows with the bulk stream.

The model under steady-state and isothermal regime is based on the following assumptions:

(1) Reactor geometry is cylindrical.
(2) No radial convection in the thin membrane and the spongy matrix.
(3) Single catalytic reaction occurs in the spongy matrix (A + B ↔ Products).
(4) Skin membrane is inert and the reaction occurs only in the spongy matrix.
(5) Constant effective diffusion coefficients in the membrane and spongy region.
(6) When dense membrane (non-porous polymer) is considered, partition coefficients at both membrane faces are constant.
(7) At $r = d$, an impermeable wall exist.

Thus, the governing equation for the inert membrane (see Fig. 1) can be written as:

$$\frac{D_{\text{efm}}}{r}\frac{\mathrm{d}}{\mathrm{d}r}r\frac{\mathrm{d}C}{\mathrm{d}r} = 0, \quad a \le r \le b \tag{1}$$

where D_{efm} and C denote effective diffusion coefficient and concentration of the key component in the membrane, respectively. Eq. (1) must be integrated with boundary conditions:

$$C = C_a \quad r = a, \qquad C = C_b \quad r = b \tag{2}$$

Solving differential equation (1), the mass balance can be conveniently written in the following fashion:

$$k_{\text{L}}(C_0 - C_a)2\pi a\,\mathrm{d}z = \frac{D_{\text{efm}}(C_a - C_b)}{a\ln(b/a)}2\pi a\,\mathrm{d}z = \eta R(b)\pi(d^2 - b^2)\,\mathrm{d}z \tag{3}$$

where η is the effectiveness factor for the spongy matrix region, $R(b)$ the intrinsic reaction rate per unit spongy matrix volume, evaluated at $r = b$, ($C = C_b$) and k_{L} is the mass transfer coefficient in the lumen, that will depend upon fluidynamic conditions.

By introducing:

$$B = \eta R(b)(d^2 - b^2) \tag{4}$$

and taking into account Eq. (3), the unknown concentrations C_a and C_b can be calculated as

$$C_a = C_0 - \frac{B}{2k_{\text{L}}a} \tag{5}$$

$$C_b = C_0 - \frac{B}{2}\left[\frac{1}{k_{\text{L}}a} + \frac{\ln(b/a)}{D_{\text{efm}}}\right] \tag{6}$$

The procedure can also be applied when the thin membrane is a dense (non-porous) polymer. The concentration profile as a function of the fiber radius will be discontinuous at the lumen–membrane and membrane–spongy region interfaces. The equilibrium partition coefficients:

$$K^a = \frac{C_{\text{am}}}{C_a} \quad \text{and} \quad K^b = \frac{C_{\text{bm}}}{C_b} \tag{7}$$

provide the relation between interface concentration membrane side and lumen or spongy matrix side, respectively. In this case the equation to estimate C_a (Eq. (5)) will be the same but:

$$C_{\text{am}} = K^a C_a \quad \text{and} \quad C_b = K^a C_0 - \frac{B}{2}\left[\frac{K^a}{k_{\text{L}}a} + \frac{\ln(b/a)}{D_{\text{efm}}}\right] \tag{8}$$

Eqs. (5) and (6) or (5) and (8) must be used to simulate reactor performance and concentration profile calculation along the reactor coordinate (z). Usually at each point along z, the non-linear second order differential mass balance within the spongy matrix must be numerically solved to estimate the flux and hence parameter B. In this contribution an approximate procedure recently presented by the authors will be used.

To obtain η the dimensionless mass balance differential equation in the spongy matrix region:

$$\frac{1}{x}\frac{\mathrm{d}}{\mathrm{d}x}x\frac{\mathrm{d}C^*}{\mathrm{d}x} = \phi^2 R^*(C^*) \tag{9}$$

should be solved subject to the following dimensionless boundary conditions:

$$C^* = 1 \text{ at } x = \alpha \quad \text{and} \quad \frac{\mathrm{d}C^*}{\mathrm{d}x} = 0 \text{ at } x = 1 \tag{10}$$

Where the following dimensionless variables were defined:

$$x = \frac{r}{d}, \qquad C^* = \frac{C}{C_b}, \qquad R^*(C^*) = \frac{R(C)}{R(C_b)} \tag{11}$$

and

$$\phi^2 = \frac{d^2 R(C_b)}{D_{\text{ef}}C_b} \tag{12}$$

denotes Thiele modulus while $\alpha = b/d$

By definition:

$$\eta = \frac{\int_\alpha^1 R^*(C^*)x\,\mathrm{d}x}{\int_\alpha^1 x\,\mathrm{d}x} = \frac{2\int_\alpha^1 R^*(C^*)x\,\mathrm{d}x}{1 - \alpha^2} \tag{13}$$

However, from Eq. (9):

$$x\frac{\mathrm{d}C^*}{\mathrm{d}x}\bigg|_\alpha^1 = \phi^2\int_\alpha^1 R^*(C^*)x\,\mathrm{d}x \tag{14}$$

Now, taking into account conditions (10) and Eq. (14):

$$\eta = -\frac{2\alpha}{(1-\alpha^2)\phi^2}\left.\frac{dC^*}{dx}\right|_{\alpha} \tag{15}$$

The matching expression proposed by Gottifredi et al. [16] is used to fit asymptotic expressions for large and small ϕ values:

$$\eta = [\phi^{*2} + \exp(-\delta\,\phi^{*2})]^{-1/2} \tag{16}$$

where

$$\phi^* = \frac{\phi}{P}, \qquad P = \frac{2\alpha}{1-\alpha^2}\rho \tag{17}$$

$$\rho = \left[2\int_0^1 R^*(C^*)dC^*\right]^{1/2} \tag{18}$$

and

$$\delta = 1 - 2\sigma^*, \quad \sigma^* = -\frac{2R^{*'}(1)\alpha^2}{(1-\alpha^2)^3}\rho^2\left[\frac{3}{4} + \frac{\alpha^4}{4} - \alpha^2 + \ln\alpha\right] \tag{19}$$

$R^{*'}(1)$ denotes $R^*(C^*)$ derivative evaluated at $C^* = 1$. Effectiveness factor calculation along reactor axial position can now be carried out through a very simple and accurate algebraic routine avoiding the numerical solution of Eq. (9). It must be stressed that $R^*(C^*)$ describes any arbitrary kinetic expression [15].

3. Hollow fiber bioreactor simulation (design equation)

Using the heterogeneous one-dimensional model [17], accounting for interfacial, intra-membrane and intra-spongy phase gradients, the key component conversion (X) over an elementary bioreactor volume may now be written as

$$\frac{dX}{dz} = \Omega\eta(C_b)R(C_b)\frac{R_V}{F^\circ} \tag{20}$$

where Ω, R_V and F° are the bioreactor total cross section, the spongy region to total reactor volume ratio and the key component entrance molar feed rate, respectively. It must be noticed that the appropriate definition of η allows dealing with a plug flow homogeneous reactor. Since in η calculation the interphase mass transfer coefficient k_L and the driven force, difference between the mixing cup concentration C_0 in the fluid phase and the concentration on the inert membrane C_a, is taken into account.

This equation must be solved subject to the following conditions:

$$C_0 = C_0^0(X = 0) \text{ at } z = 0 \tag{21}$$

where

$$C_0 = C_0^0(1 - X)$$

C_0^0 denotes key component mixing cup concentration at the reactor entrance. It should be stressed that C_b can only be found through an algebraic trial and error procedure. So

1. Start at the reactor entrance. At this position it is assumed $C_b = C_0^0$.
2. With Eq. (16), the effectiveness factor η is calculated since all the parameters are known.
3. With Eqs. (4)–(6), B, C_a and C_b are calculated (or either with Eqs. (5) and (8)).
4. With this value of C_b a correction is made with Eqs. (16), (4), (5) and (6) (or Eqs. (5) and (8)).
5. The whole procedure is repeated until two successive calculations of C_b indicate the desired convergence has been achieved.
6. The next step of the Runge-Kutta procedure on Eq. (20) is speeded up using the values of η, C°, C_a and C_b found in the previous step as first guess.

Therefore, the values of C_0, C_a, C_b, η and X along the reactor are obtained and the complete simulation of bioreactor done. As can clearly be seen the numerical solution of the second order non-linear differential mass balance (Eq. (9)), is avoided and replaced by an algebraic rapidly convergent method.

4. Results and discussion

It must be stressed that the method developed in this contribution reduces the prediction of the membrane reactor performance to a well-known plug flow reactor in which an algebraic equation must be solved in each step of the integration interval.

The usual problems associated with the numerical integration of a non-linear second order differential equation, with boundary values, are completely overcome with an early procedure of the authors [15] applied to the specific geometry of a hollow fiber bioreactor.

Jayaraman and Kulkarni [11] presented a numerical procedure to predict the performance of a hollow fiber membrane reactor assuming fully developed laminar flow in the core and Michaelis–Menten expression to describe the catalytic kinetics into the spongy region. The final expression implies the numerical solution of an integro differential equation (Volterra type) together with the numerical integration, in each step, of the differential mass balance equation (9). They claim that numerical integration can be easily performed with standard shooting method routines. This is only true when mild concentration profiles in the spongy region are met (i.e. ϕ is small). But even in such a case the procedure of solving the reaction diffusion equation at each step is quite time consuming. With our procedure, instead, a non-linear algebraic equation must be solved at each step where, in all cases, the initial guess is nearby the true solution.

Conversion profiles estimated with our simple procedure are presented in Fig. 2 as continuous lines. Michaelis–Menten kinetic expression (see Eq. (22)) was used in this simulation with two values of V_m. Both curves reflect the influence of increasing the rate of reaction while keeping the other parameter fixed. As can be seen conversion increases as V_m increases at each axial position along the reactor although the slope clearly shows the influence of the decaying driving force as reactive consumption approaches 90%. In the same Fig. 2, for comparison purposes,

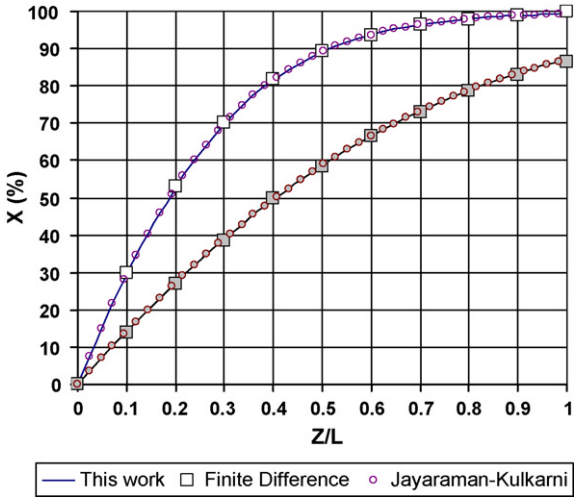

Fig. 2. Substrate concentration axial profiles. Conditions: $(K_m/C_0^0) = 1$; $d/b = 1.5$; $D_{ef}/D_{efm} = 10$; $k_L = 10^{-4}$ m/s; $F^\circ = 7.85 \times 10^{-10}$ mol/s. Upper curve: $V_m = 0.655$ mol/m^3 s (open symbols). Underneath Curve: $V_m = 0.295$ mol/m^3 s (close symbols).

values predicted by Jayaraman and Kulkarni [11] (circles) and with finite difference method (squares) are also shown. As can be seen our simple procedure is very accurate since no noticeable differences are observed.

5. Application

The procedure was also applied to simulate the behavior of a relevant industrial process performed in membrane reactors. Drioli and Giorno [2] mentioned this type of reactor in the case of industrial production of lactic acid using biocatalysts.

Hooijmans et al. [18] carried out experiments for determining the intrinsic kinetic parameters of an agarose-gel immobilized oxygen consuming enzyme: L-lactate 2-monooxygenase. The reaction rate on the enzyme is well described by Michaelis–Menten kinetics since oxygen is the sole rate limiting substrate:

$$R(C) = \frac{V_m C}{K_m + C} \tag{22}$$

The kinetic parameters values obtained at 37 °C for the reaction:

$$CH_3–CHOH–COOH + O_2 \rightarrow CH_3–COOH + CO_2 + H_2O$$

are $V_m = 6 \times 10^{-2}$ mol/m^3 s, $K_m = 0.05$ mol/m^3

Authors [18] also reported oxygen effective diffusivity in the agarose support ($D_{ef} = 2.3 \times 10^{-9}$ m^2/s). To perform the reactor performance simulation a number of assumptions have been introduced: oxygen effective diffusivity in the skin ($D_{efm} = 3 \times 10^{-10}$ m^2/s), geometry reactor parameters ($a = 1 \times 10^{-4}$ m; $b = 1.05 \times 10^{-4}$ m; $d = 1.75 \times 10^{-4}$ m, $L = 0.2$ m), liquid flow rate ($Q = 1.57 \times 10^{-9}$ m^3/s). Thus a Reynolds number of around 10 results with a pressure drop of 40 kPa. A film mass transfers coefficient (k_L) of 4.4×10^{-5} m/s was assumed, after Hooijmans et al. [19]. The initial oxygen concentration was 0.7 mol/m^3.

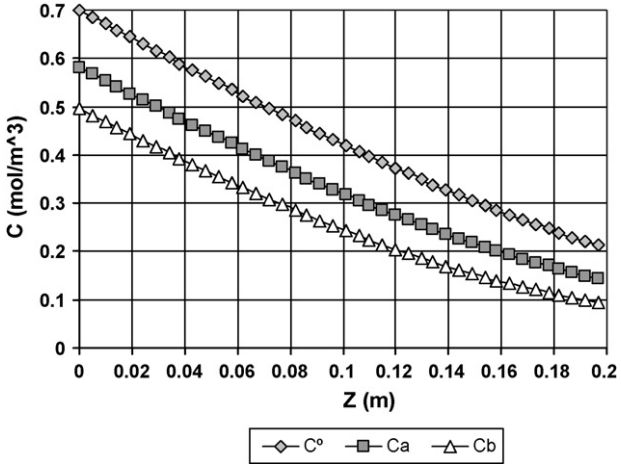

Fig. 3. Concentration profiles along the membrane reactor axial coordinate.

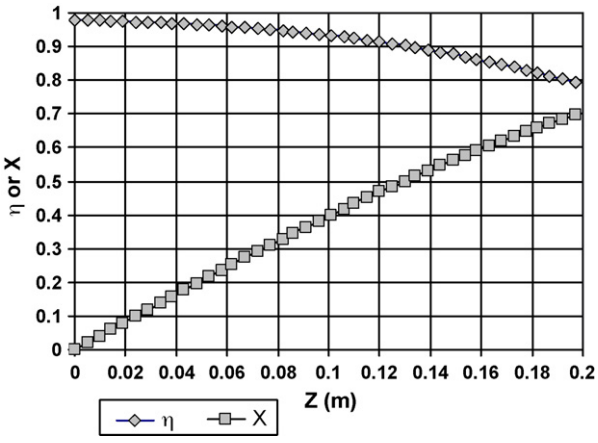

Fig. 4. Effectiveness factor and conversion along the membrane bioreactor.

Bulk oxygen concentration profiles in the lumen (C_0), at the skin–lumen interface (C_a) and skin–spongy interface (C_b) as predicted with our procedure are presented in Fig. 3. It is clearly seen that concentration ratios (C_0/C_a, C_0/C_b) increases along the reactor axial position to sustain oxygen consumption in the spongy region although C_b is also decaying. As a consequence while conversion increases η, as a global effectiveness reaction factor, decreases along the reactor flow coordinate. This is clearly shown in Fig. 4 where η and conversion results are plotted as function of z. In this particular case the reaction rate is small in comparison with rate of oxygen diffusion in the spongy region. Nevertheless η decreases as driving force for the whole process decreases because it was defined as a global coefficient taking into account concentration depletion between bulk and spongy interfaces.

6. Conclusions

A simple, rigorous and accurate procedure to simulate a hollow fiber membrane biocatalytic reactor has been proposed. With the introduction of an appropriate definition of an overall effectiveness factor, that takes into account the effect of the chemical consumption as well as mass transfer resistances, mass balance

of key component in the reactor is reduced to the well-known plug flow packed bed catalytic reactor [17].

It can be applied to any biocatalytic system provided the kinetic behavior can be described by a single chemical reaction although there is no limitation regarding the complexity of the resulting kinetic expression. The usual instabilities and stiffness associated with the numerical solution of the non-linear second order, boundary values, differential equation [20] are completely overcome with the proposed procedure since η is estimated through an algebraic equation.

The outcoming results expressed in terms of conversion profiles along the reactor show a fair agreement with previous findings obtained by numerical solution of the reaction diffusion equation in the spongy region where the catalyst is immobilized.

A biocatalytic reaction system previously investigated to study enzyme immobilization were used to simulate a hollow fiber reactor assuming some geometrical parameters but with kinetic parameters reported in the contribution [18]. Membrane reactor simulation takes a few seconds and conversion profiles can be easily generated as function of reactor axial coordinate.

The effect of mass transfer resistances can also be seen by plotting the concentration profiles at each boundary of the hollow fiber and also the corresponding effectiveness factor values. It shows that radial mass transfer rates decrease along the reactor which causes a similar effect on the overall effectiveness factor. This behavior does not match with the usual plug flow packed bed reactor where η increases with conversion along the reactor.

It is expected that the present contribution will be useful to analyze and simulate membrane biocatalytic reaction both for research and scale up purposes even in those cases where the catalyst is not uniformly distributed in the spongy region [15].

Acknowledgements

Authors wish to thank Consejo Nacional de Investigaciones Científicas y Técnicas (CONICET), Agencia Nacional de Promoción Científica y Tecnológica (ANPCYT) and Universidad Nacional de Salta for financing this Project (Grant 1411700).

References

[1] G. Belfort, Membranes and bioreactors: a technical challenge in biotechnology, Biotechno1. Bioeng. 33 (1989) 1047–1066.
[2] E. Drioli, L. Giorno, Biocatalytic Membrane Reactors, Taylor & Francis Ltd, London, 1999.
[3] Y. Kourkoutas, A. Bekatorous, I.M. Banat, R. Marchant, A.A. Koutinas, Immobilization technologies and support materials suitable in alcohol beverages production: a review, Food Microbiol. 21 (2004) 377–397.
[4] P.S. Sehanputri, C.G. Hill Jr., Biotechnology for the production of nutraceutical enriched in conjugated linoleic acid. I. Uniresponse kinetics of the hydrolysis of corn oil by *Pseudomonas* sp. Lipase immobilized in hollow fiber reactors, Biotechnol. Bioeng. 64 (1999) 568–579.
[5] P.R. Rony, Multiphase catalysis II. Hollow fiber catalysts, Biotechnol. Bioeng. 13 (1971) 431–443.
[6] P.R. Rony, Hollow fiber enzyme reactors, J. Am. Chem. Soc. 94 (1972) 8247–8256.
[7] W. Tischer, F. Wedekind, Immobilized enzymes: methods and applications, Top. Curr. Chem. 200 (1999) 95–126.
[8] E. Gonzalez Días, R. Catana, B.S. Ferreira, S. Luque, P. Fernández, J.M.S. Cabral, Towards the development of a membrane reactor for enzymatic inulin hydrolysis, J. Membr. Sci. 273 (2006) 152–158.
[9] M.I. Cabrera, J.A. Luna, R.J. Grau, Solving design equations for a hollow fiber bioreactor with arbitrary kinetics, Chem. Eng. J. 84 (2001) 445–461.
[10] V.K. Jayaraman, Solution of hollow fiber bioreactor design equations for zero order limit of Michaelis–Menten kinetics, Chem. Eng. J. 51 (1993) 363–366.
[11] V.K. Jayaraman, B.D. Kulkarni, An efficient algorithm for solving hollow fiber bioreactor design equations, Chem. Eng. J. 65 (1997) 77–80.
[12] J.M. Sousa, A. Mendes, Simulating catalytic membrane reactors using orthogonal collocation with spatial coordinate transformation, J. Membrane Sci. 243 (2004) 283–292.
[13] L.R. Waterland, A.S. Michaels, C.R. Roberson, A theoretical model for enzymatic catalysis using asymmetric hollow fiber membranes, AIChE J. 20 (1974) 50–59.
[14] R.N. Pavnovic, Z.Z. Zarago, M.N. Tepic, Analysis of a model hollow fiber bioreactor wastewater treatment, Chem. Eng. Sci. 48 (1993) 1069–1075.
[15] J.C. Gottifredi, E.E. Gonzo, On the effectiveness factor calculation for a reaction-diffusion process in an immobilized biocatalyst pellet, Biochem. Eng. J. 24 (2005) 235–242.
[16] J.C. Gottifredi, E.E. Gonzo, O.D. Quiroga, Effectiveness factor calculations, in: Whitaker, Cassano (Eds.), Concepts and Design of Chemical Reactors, Gordon and Breach Publisher, 1987.
[17] K. Bischoff, G. Froment, Chemical Reactor Analysis and Design, Wiley, New York, 1980.
[18] C.M. Hooijmans, M.L. Stoop, M. Boon, K.C.A.M. Luyben, Comparison of two experimental methods for the determination of Michaelis–Menten kinetics in an immobilized enzyme, Biotechnol. Bioeng. 40 (1992) 16–24.
[19] C.M. Hooijmans, S.G.M. Geraats, K.C.A.M. Luyben, Use of an oxygen microsensor for the determination of intrinsic kinetic parameters of an immobilized oxygen reducing enzyme, Biotechnol. Bioeng. 35 (1990) 1078–1087.
[20] Y.M. Sun, S.-J. Khang, A catalytic membrane reactor: its performance in comparison with other types of reactors, Ind. Eng. Chem. Res. 29 (1990) 232–238.
[21] S.S. Kim, D.O. Cooney, An improved theoretical model for hollow fiber enzymatic reactors, Chem. Eng. Sci. 31 (1976) 289–294.